Proximity effect in electronbeam lithography

T. H. P. Chang

Citation: J. Vac. Sci. Technol. **12**, 1271 (1975); doi: 10.1116/1.568515
View online: http://dx.doi.org/10.1116/1.568515
View Table of Contents: http://avspublications.org/jvst/cresource/1/JVSTAL/v12/i6
Published by the AVS: Science & Technology of Materials, Interfaces, and Processing

Proximity effect in electron-beam lithography

T. H. P. Chang

IBM Thomas J. Watson Research Center, Yorktown Heights, New York 10598

(Received 28 August 1975)

A simple technique for the computation of the proximity effect in electron-beam lithography is presented. The calculations give results of the exposure intensity received at any given point in a pattern area using a reciprocity principle. Good agreement between the computed results and experimental data was achieved.

PACS numbers: 85.40.C, 84.80.D, 07.72., 79.20.K

INTRODUCTION

The proximity effect in electron-beam lithography is the name given to the well known phenomena that a uniform exposure by the incident beam can give rise to a nonuniform distribution of actually received exposure in the pattern area. This nonuniformity can be characterized in two ways: (1) a variation between pattern elements and (2) a variation inside a pattern element. In the first case, the nonuniformity varies partly with the geometries (e.g., linewidth) of the pattern elements and partly with the distribution (spacings and sizes) of the adjacent pattern elements. In general, a smaller pattern element receives less exposure than a larger one, and an isolated element receives less exposure than one in a packed area. In the second case, the exposure received in the center of a pattern element is generally higher than that on the edges, typically 2 times higher in the case of a wide isolated line (linewidth $>10\ \mu$m). As a result of the proximity effect, the pattern definition would suffer different degrees of deterioration. For example, lines in a highly packed area would become wider than intended and in the worse case they might even merge together.

The proximity effect is created by the backscattered electrons which introduce exposures away from the point of beam incidence. The effect is therefore dependent on the beam accelerating voltage, the resist material and thickness, substrate material, the resist contrast characteristics, and the chemical development process used. Where the beam diameter is appreciable then the current-density profile of the beam must also be considered.

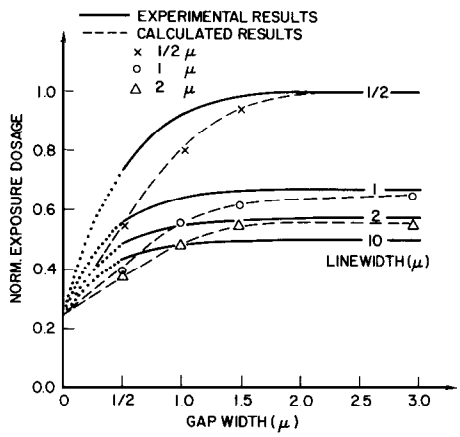

FIG. 1. Variation of exposure dosage with linewidth and gap width.

Figure 1 shows the experimental results (solid lines) of the variation of exposure requirements with pattern linewidth and packing density (i.e., gap width). It can be seen that the importance of the proximity effect increases with a decrease of linewidth and gap width. In general, for linewidth and gap $>2\ \mu$m the variation of exposure dosage is relatively small and can, in general, be taken care of by the resist exposure latitude. However, for linewidth and gap width in the micron and submicron range, this variation of exposure requirement can become significant. For example, a 30% variation of exposure is required when comparing 1- and 0.5-μm lines at a gap width $>3\ \mu$m, and a 45% exposure variation is required for 1-μm lines at a 0.5-μm gap as compared with 0.5-μm lines at >3-μm gaps.

To achieve accurate pattern delineation, it is therefore necessary to apply some method of exposure adjustment to compensate for the proximity effect. One such method is to vary the scanning speed of each pattern element.[1,2] This method is particularly suitable for vector-scan exposure technique[3] where the pattern is first decomposed into a series of smaller elements and the electron beam exposes each of these elements sequentially by a fill-in scan. This technique can also be combined with a framing or spiral fill-in scan[3] to achieve additional compensation for the variation of exposure inside the element.

In a computer-controlled electron-beam system, such exposure adjustments can be readily applied automatically. There is therefore a need to develop a method by which these variations of exposure requirements over the pattern area can be readily evaluated. The following is a description of one such method which employs a reciprocity principle to simplify the calculation. Results computed from this principle have been compared with experimental values.

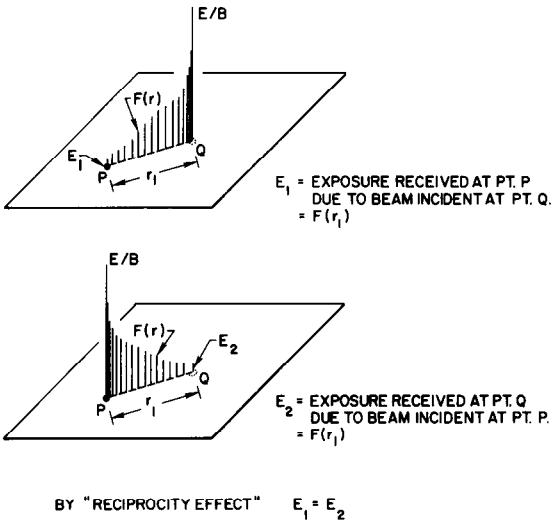

FIG. 2. (a) Exposure E_1 received at point P due to beam incident at point $Q=F(r_1)$. (b) Exposure E_2 received at point Q due to beam incident at point $P=F(r_1)$.

THE RECIPROCITY PRINCIPLE

When an electron beam is incident at a point Q on the surface of the wafer it will introduce a rotationally symmetric zone of exposure around this point of incidence with an intensity distribution which decreases with increase of radial distance as shown symbolically in Fig. 2(a). The exposure intensity E_1 received at a point P, radial distance r_1 away from point Q, is given by

$$E_1=F(r_1),$$

where $F(r)$ is the function describing the exposure intensity distribution (EID).

If the beam is now shifted to point P as shown in Fig. 2(b), the corresponding exposure intensity E_2 received at point Q will be given by

$$E_2=F(r_1).$$

Obviously $E_1=E_2$.

This relationship is the basis of the "reciprocity principle" which says that the exposure introduced at point P by a beam incident at point Q is the same as the exposure received at point Q, if the beam is shifted to point P.

This reciprocity principle can be applied to the case where the beam is incident at a number of points, Q_1, Q_2, Q_3, etc. as shown in Fig. 3. The exposure intensity received at point P due to these multiple beam incidences can be obtained by simply assuming the beam to be incident at point P and summing the corresponding exposure intensities received at points Q_1, Q_2, Q_3,

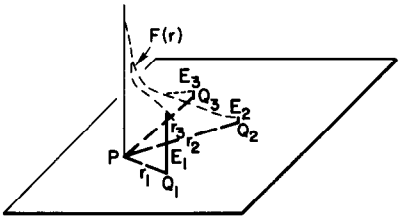

FIG. 3. Exposure E_p received at point P due to beam incidence at Q_1, Q_2, Q_3, etc. $=E_1+E_2+E_3+\cdots=\sum_{k=1}^{n}F(r_k)$.

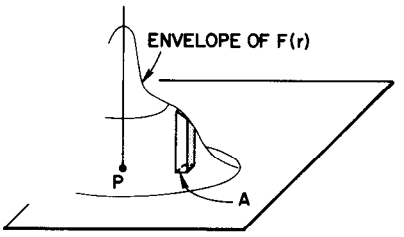

FIG. 4. Exposure E_p received at point P due to the beam incidence over area A $=\int_A F(r)\Delta A=$ shaded volume.

etc.,

$$E_p=\sum_{k=1}^{n}F(r_k).$$

Similarly, in the case where the electron-beam exposure is uniformly distributed over a given area A as shown in Fig. 4, the exposure received at point P due to this distributed source can again be obtained by assuming the beam to be incident at point P and the integrated sum of the corresponding exposures received over the given area A

$$E_p=\int_A F(r)dA.$$

This is given by the shaded volume under the EID curve as shown in Fig. 4.

In the case where multiple areas are scanned, as shown in Figs. 5(a) and 5(b), the exposure received at a point P can be obtained by simply summing the volumes as defined by each of these scanned areas under the EID curve. In Figs. 5(a) and 5(b), the exposure is evaluated for the two points of interest, P_1 and P_2, respectively, and it can be seen from the difference in volumes under the EID curve that ex-

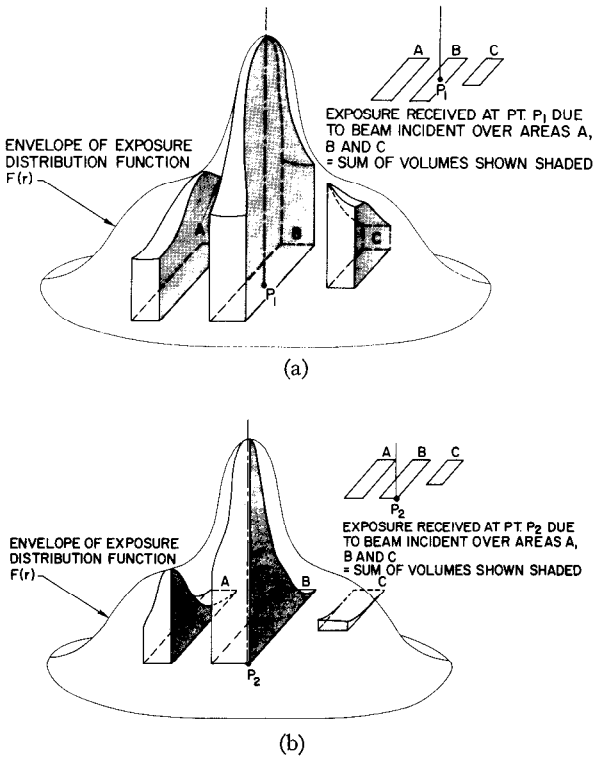

FIG. 5. Envelopes of exposure distribution function $F(r)$. (a) Exposure received at point P_1. (b) Exposure received at point P_2.

posure intensity received at P_1 is considerably greater than that at P_2.

It follows from the above discussions that a simple method for the computation of proximity effect can be formulated as follows: The exposure received at any given point P in the pattern field can be evaluated by two simple procedures:

(1) Shift the origin of the EID curve to the point P, where the exposure is to be evaluated.

(2) Compute the exposure intensity received at this point P by

$$E_p = \Sigma \int F(r)dA,$$

which is the volume as defined by all the exposed areas under the EID curve.

For example, in the case of exposing a large rectangular pad with sides larger than that of the range of the backscattered electrons, say a 10×10-μm pad, the exposure received at the center of the pad will be given by

$$E_1 = \text{total volume under the EID curve};$$

the exposure received at the midpoint along the edge of the pad

$$E_2 = \tfrac{1}{2}(\text{total volume under the EID curve}) = \tfrac{1}{2}E_1;$$

the exposure received at the corner of the pad

$$E_3 = \tfrac{1}{4}(\text{total volume under the EID curve}) = \tfrac{1}{4}E_1.$$

This means that the exposure intensity over the pad area is nonuniform. The center of the pad received exposure twice that at the edge and four times that at the corner.

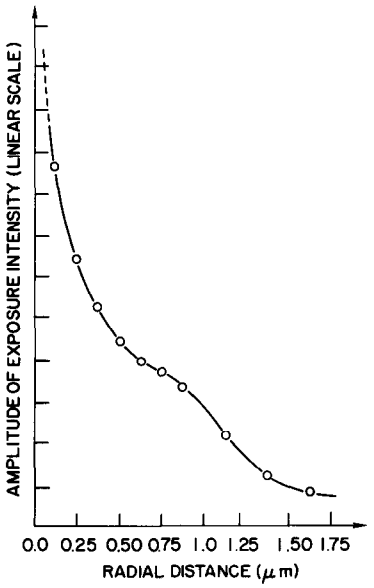

FIG. 6. Exposure intensity distribution obtained experimentally using a 25-kV 0.2-μm-diam incident beam on a silicon substrate with a 6000-Å PMMA resist developed in MIBK:isopropyl alcohol (1:1) for 60 sec. The exposure intensity distribution approximates the sum of two Gaussian distributions: $C_1\exp(-r^2/B_1^2)$ for primary electrons and $C_2\exp(-r^2/B_2^2)$ for BS electrons. For best fit, $B_1=0.1$–0.2 μm; $B_2=1$–1.2 μm, and $C_1/C_2=1.5$–3.

THE EXPOSURE INTENSITY DISTRIBUTION

The radial exposure intensity distribution introduced by a point source of electrons can be evaluated either analytically or experimentally. The analytical techniques applicable to this evaluation include the well known Monte Carlo technique[4,5] and other analytical models.[6]

A relatively simple experimental technique will be described here to show how a first-order study of the EID can be conducted. The experiment used a computer controlled E/B system to generate a special test pattern which consisted of a series of small isolated rectangles. The sizes of these rectangles vary from 0.25 to 10 μm on a side in progressively increasing order at 0.25-μm increments. A number of these patterns were exposed at different exposure dosages on the same wafer, and the pattern was then developed in a controlled manner. The resultant patterns were examined under a microscope to determine the exposure dosage value required to clear the center of each rectangular element. These values can be deconvoluted applying the computing technique based on the "reciprocity principle" described earlier, to obtain the EID curve.

Figure 6 shows the experimentally obtained result of the EID of a 25 kV beam incident on a silicon wafer covered with 6000 Å of PMMA resist and developed with a 1:1 developer (MIBK:IPA) at room temperature for 60 s. It can be seen that the EID can be closely approximated by the sum of two Gaussian distributions:

$C_1\exp[-(r/B_1)^2]$ incident primary beam,

$C_2\exp[-(r/B_2)^2]$ backscattered electrons;

and for best fit, the values of the constants are

$$B_1 \simeq 0.1\text{–}0.2\ \mu\text{m},$$
$$B_2 \simeq 1\text{–}1.2\ \mu\text{m},$$
$$C_1/C_2 \simeq 1.5\text{–}3.$$

This result indicates that the zone of exposure introduced by the backscattered electrons is approximately 2–3 μm in radius for a 25 kV beam and the exposure intensity introduced by the backscattered electrons at the center is approximately 20 to 30% of the total exposure.

This distribution will vary with beam operating voltage, resist and substrate materials, and the development technique.

COMPARISON WITH EXPERIMENTAL RESULTS

The following cases have been studied using the "reciprocity principle" and the experimentally obtained EID curve. A computer program was written assuming the EID curve to be composed of two Gaussian distribution curves as described earlier. This program allows a complex pattern to be entered as a series of rectangles

TABLE I. Isolated lines exposure received on the edges of the lines. ( )—Exposure compensation required.

Linewidth	Experimental results	Calculated results
½ μm	1 (1)	1 (1)
1 μm	1.50 (0.67)	1.55 (0.65)
2 μm	1.75 (0.57)	1.81 (0.55)

in much the same way as the pattern data are arranged for electron beam exposure in the vector-scan technique. The computer results give the exposure intensity received at the points considered, and they are then compared with the experimental data. In all the cases, experiments were performed with 25 kV accelerating potential on PMMA resist on silicon.

Case 1: Single isolated line

Three different linewidths were considered, 0.5, 1, and 2 μm. The computations were performed by assuming the line to be infinitely long and the EID curve was placed at the edge of the line. Experiments were performed using a computer-controlled electron-beam system to expose the required lines. A wide range of exposure dosage was applied and the correct exposure condition for each line verified. Table I shows the results obtained using these two approaches and in each case the value for the 0.5-μm line was used as the reference. It can be seen that good agreement was achieved between the computed results and the experimental data.

Case 2: Groups of lines

The computational approach was applied to groups of lines. In each group the lines have identical linewidth and spacing. A series of these groups was studied with the linewidth varying from 0.5 to 10 μm, and spacings (measured as the clear gap width between two neighboring lines) varying from 0.5 to 3 μm at 0.5-μm increments. In each group, the EID curve was placed at the edge of a line at the center of the group, and the length of the lines were taken as infinite. Similar groups of lines were also exposed in the electron beam system, and the correct exposure for each group ascertained. It should be pointed out that some difficulties were experienced in determining the correct exposure in the experiments because a range of exposure may be considered acceptable. The average value was taken here as the representative value. In both approaches, all exposure values were normalized with the value of 0.5-μm lines group taken as 1.

Figure 1 shows the results. The dotted lines give the computational results and the solid lines give the experimental values. It can be seen that reasonable agreement between the two approaches was achieved, in particular for lines at larger gap spacings. At smaller gaps, the difficulties in establishing the correct exposure value experimentally as mentioned earlier may account for some of the discrepancies. It can be noticed that all the curves in the figure converge to a point on the axis where the gap width is zero. The normalized exposure value of this point is shown as half of the 10-μm lines at 3-μm gap width. The reason for this can be easily explained by the fact that as the gap width approaches zero the exposure requirement would decrease progressively to the condition for the center of a big pad. It has been shown that exposure value received in the center of a big isolated pad is twice that received at the edges. The 10-μm wide lines at 3-μm gap width are taken here as equivalent to a big isolated pad, hence the converging point is established.

Case 3: T-I bars vs chevrons in bubble pattern exposures

T-I bars and chevrons are two commonly used shapes in bubble technology. Because of the difference in their packing density (the chevrons are much more highly packed as compared to the T-I bars), it was found in practice that some adjustments in exposure dosage were needed to compensate for this difference. Experimentally, a 10% adjustment was found necessary for 1-μm linewidth patterns containing these two geometries. Figure 7 shows the typical layout of these two elements in a circuit. The computational approach is used to map out the equi-exposure contour lines for each of these elements. To achieve this, the EID curve is positioned at a matrix of points over each of these elements, and the presence of the surrounding elements accounted for by computing the volume under the EID curve for each position. The computed values give the exposure received at that point which may be inside or outside the element boundaries. Knowing these values, one can generate the equi-exposure contour lines either manually or by a computer program. Figure 7 also shows one such computed equi-exposure line; the one nearest to the pattern boundaries for each case and this would represent the outline of the pattern when developed. It can be seen that for the case of T-I bars, the value of the equi-exposure line is 5.5, and the corresponding value for the chevron is 6.2. The ratio of these two values is 0.89 which represents an 11% compensation requirements, and it agrees well with the 10% value found experimentally.

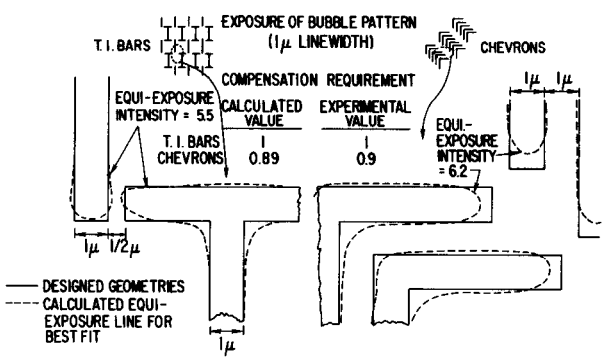

FIG. 7. Exposure of bubble pattern (1-μm linewidth).

CONCLUSION

The importance of taking proper consideration of the proximity effect in electron-beam lithography is well established, and the need to apply compensation for this effect for high-resolution patterns has been demonstrated. A computation technique based on a reciprocity principle is introduced. This technique can be used to calculate the exposure intensity received at any point in the pattern area by the use of the exposure intensity distribution curve of a point source. The EID curve can be generated either analytically or experimentally as discussed in the paper. The experimentally generated EID curve was found to approximate the sum of two Gaussian-distribution curves which considerably simplifies the computation. The computation technique has been used to study several cases of pattern exposures where experimental results also exist, and good agreement was achieved. The technique may be used as an aid to compute the compensation requirements for the proximity effect in complex patterns and can be part of the pattern data preparation programs. Such compensation information is particularly valuable to the vector-scan electron beam system where exposure conditions over the pattern area can be readily adjusted.

ACKNOWLEDGMENTS

The author gratefully acknowledges the technical contributions of A. D. Wilson, A. Speth, A. Kern, W. W. Blair, L. Keller, and H. Luhn and many helpful discussions with A. N. Broers and M. Hatzakis. The computer programs used for the sample calculations were prepared by E. Munro and M. Parikh, and their contributions are much appreciated.

[1]F. S. Ozdemir, W. E. Perkins, R. Yim, and E. D. Wolf, J. Vac. Sci. Technol. **10**, 1008 (1973).
[2]T. H. P. Chang, A. D. Wilson, A. Speth, and A. Kern, *Proceedings of the 6th International Conference on Electron and Ion Beam Science and Technology 1974*, edited by R. Bakish (Electrochemical Society, Princeton, NJ, 1974).
[3]T. H. P. Chang, A. Speth, A. D. Wilson, and A. Kern, "Electron Beam Lithography using Vector Scan Technique," 13th Symposium on Electron, Ion and Laser Beam Technology, 1975.
[4]D. Kyser and K. Murata, see Ref. 2.
[5]R. Hawryluk, A. Hawryluk, and H. Smith, J. Appl. Phys. **45**, 2551 (1974).
[6]J. Greeneich and T. Van Duzer, IEEE Trans. Electron Devices, **ED-21**, 286 (1974).